ORIGINAL ARTICLE

Base-to-apex Gradient Pattern Assessed by Cardiovascular Magnetic Resonance in Takotsubo Cardiomyopathy

Riccardo Cau,* Giuseppe Muscogiuri,†‡ Vitanio Palmisano,§
AQ2 Michele Porcu,* Alessandra Pintus,* Roberta Montisci,‖ Lorenzo Mannelli,¶
Jasjit S. Suri,# Marco Francone,** and Luca Saba*

Objectives: The purpose of this study was to investigate the base-to-apex gradient strain pattern as a noncontrast cardiovascular magnetic resonance (CMR) parameter in patients with Takotsubo cardiomyopathy (TTC) and determine whether this pattern may help discriminate TTC from patients with anterior myocardial infarction (AMI).

Materials and Methods: A total of 80 patients were included in the analysis: 30 patients with apical ballooning TTC and 50 patients with AMI. Global and regional ventricular function, including longitudinal (LS), circumferential (CS), and radial strain (RS), were assessed using CMR. The base-to-apex LS, RS, and CS gradients, defined as the peak gradient difference between averaged basal and apical strain, were calculated.

Results: The base-to-apex RS gradient was impaired in TTC patients compared with the AMI group (14.04 ± 15.50 vs. -0.43 ± 11.59, $P = 0.001$). Conversely, there were no significant differences in the base-to-apex LS and CS gradients between the AMI group and TTC patients (0.14 ± 2.71 vs. -1.5 ± 3.69, $P = 0.054$: -0.99 ± 6.49 vs. ±1.4 ± 5.43, $P = 0.47$, respectively). Beyond the presence and extension of LGE, base-to-apex RS gradient was the only independent discriminator between TTC and AMI (OR 1.28; 95% CI 1.08, 1.52, $P = 0.006$) in multivariate logistic regression analysis.

Conclusion: The findings of this study suggest that the pattern of regional myocardial strain impairment could serve as an additional noncontrast CMR tool to refine the diagnosis of TTC. A pronounced base-to-apex RS gradient may be a specific left ventricle strain pattern of TTC.

Key Words: CMR, Takotsubo syndrome, myocardial strain, base-to-apex gradients

(*J Thorac Imaging* 2023;00:000–000)

From the *Department of Radiology, Azienda Ospedaliero Universitaria, Monserrato, Cagliari, Italy; †School of Medicine and Surgery, University of Milano-Bicocca, Milan, Italy; ‡Department of Radiology, IRCCS Istituto Auxologico Italiano, San Luca Hospital, Milan, Italy; §Ospedale General Regionale F. Miulli, Acquaviva delle Fonti, Italy; ‖Department of Cardiology, Azienda Ospedaliero Universitaria, Monserrato, Cagliari, Italy; ¶Department of Radiology, IRCCS SDN, Naples, Italy; #Stroke Diagnosis and Monitoring Division Atheropoint LLC, Roseville, CA; and **Humanitas University, Pieve Emanuele, Italy.
All authors agreed with the content and gave consent to submit.
All authors contributed equally as authors to this work.
The authors state that this work is not under consideration elsewhere
All authors read and approved the final manuscript.
Some of the patients under analysis were published in one of our previous studies.
The scientific guarantor of this publication is the corresponding author
AQ3 The authors declare no conflicts of interests.
Correspondence to: Luca Saba, MD, Department of Radiology, Azienda Ospedaliero Universitaria, di Cagliari—Polo di Monserrato s.s. 554 Monserrato,Cagliari 09045, Italy (e-mail: lucasaba@tiscali.it).

DOI: 10.1097/RTI.0000000000000761

Takotsubo cardiomyopathy (TTC) is a transient form of left ventricular (LV) dysfunction characterized by a specific pattern of LV impairment preceded by associated emotional or physical triggers.[1–3] Clinical presentation, electrocardiographic changes, and biomarkers elevation can resemble anterior myocardial infarction (AMI).[1–3] It is believed to represent ~2% of all patients presenting with suspected myocardial infarction.[4] Therefore, the differential diagnosis between the two is often challenging.[2,4] Several noninvasive imaging modalities can be useful in the workup of TTC.[1,2,5,6] Among them, cardiovascular magnetic resonance (CMR) with late gadolinium enhancement (LGE) is becoming increasingly important in the diagnosis and management of TTC,[1,2,7–10] allowing to visualize the wall motion abnormalities and the presence of reversible and irreversible myocardial damage.[7,8,11–14] In clinical practice, CMR acquisitions with LGE are often contraindicated due to the presence of concomitant renal disease.

In this scenario, CMR feature tracking (FT) is a developing noncontrast quantitative method that has demonstrated to reflect subclinical changes in myocardium contractility.[15–17]

Myocardial strain impairment has been described in patients with TTC,[5,6,18–20] including the reduction of LS, CS,[5] and impaired base-to-apex RS gradient.[21,22] The purpose of this study was to investigate the base-to-apex gradient pattern as noncontrast CMR parameters in patients with TTC and explore whether this pattern may help discriminate TTC from patients with AMI.

MATERIAL AND METHOD

Study Population

In this retrospective single-center study, we searched in our database all the patients who underwent CMR between March 3, 2017 and February 7, 2022 because of clinical suspicion of MI or apical ballooning TTC. A total of 80 subjects were finally included in the study cohort. Of those, 30 and 50 were TTC and AMI subjects, respectively.

The diagnosis of TTC was defined according to the Position Statement of the European Society of Cardiology Heart Failure Association.[23] The diagnostic criteria include regional wall motion abnormalities not limited to a single epicardial vascular distribution territory. The disease onset is usually preceded by a stressful trigger, culprit atherosclerotic coronary disease as assessed at invasive catheterization is usually absent, new ECG abnormalities are present, elevated serum natriuretic peptide and a small increase in cardiac troponin are often detected. LV dysfunction full recovery is typically noted at follow-up. Conversely, AMI was based on the presence of significant left

anterior descending coronary artery disease with more than 70% stenosis on coronary angiography with a scar pattern consistent with anterior wall myocardial infarction on CMR images.

Exclusion criteria included subjects <18 years old; contraindication to CMR (such as implantable devices, severe claustrophobia), history of renal disease with a current eGFR <30 mL/min/1.73 m2; and coronary artery disease.

The Institutional Review Board approval for this retrospective study was obtained, and the patient's consent was waived because of the retrospective nature.

A flowchart demonstrating the application of inclusion and exclusion criteria is provided in Fig. 1.

CMR Acquisition

CMR scans were performed after hospital admission with a mean delay of 4.1 ± SD 2.6 days using a 1.5 T scanner system (Philips Achieva dStream, Philips Healthcare, Best, The Netherlands). An 8-channel anterior cardiac AQ4 coil array was used. All cine-images were acquired using a balanced steady-state free precession and retrospective gating during expiratory breath-hold maneuvers (TE: 1.7 AQ5 mssec; TR: 3.4 msec/flip-angle: 45°, section thickness = 8 mm) in long-axis (2-, 3- and 4-chamber view) and short-axis plane with whole ventricular coverage from base to apex.

T2-short tau inversion recovery (T2-STIR) images were obtained using triple inversion recovery T2-weighted pulse sequence (TR = 2 RR, TE ≈ 70 msec; flip-angle: 45°, section thickness = 8 mm, FOV 300×300 mm2) in long-axis (2-, 3- and 4-chamber view) and short-axis plane with whole ventricular coverage from base to apex

T1 mapping was performed in the short-axis plane in three slices (at the base, mid-ventricular, and apex, respectively) using a single-breath-hold, ECG-triggered, MOLLI sequence before contrast media injection (TE 1.1 msec; TR 2.5 msec; flip-angle 35°; FOV, 300 × 300 mm2).

T2 mapping was acquired before the administration of contrast media on 3 representative short-axis slices (at the base, mid-ventricular, and apex, respectively) using a single-breath-hold, black-blood prepared ECG-triggered, spin-echo multiecho sequence.

LGE imaging was performed in both long and short-axis slices 10 to 12 minutes after contrast media injection (Gadovist, Bayer Healthcare, Berlin, Germany) with a dose of 0.15 ml per kg body weight using phase-sensitive inversion recovery sequences (PSIR) (TE: 2.0 msec; TR: 3.4 msec; flip-angle: 20°, section thickness = 8 mm) with an inversion time determined using the Look-Locker technique.

Image Analysis

We used the commercially available software system Circle CVI42 (CVI42, Circle Cardiovascular Imaging Inc., Calgary, Canada) for CMR-FT data analysis. Offline CMR-FT analyses were conducted for the evaluation of peak global longitudinal strain (LS), global radial strain (RS), and global circumferential strain (CS) in a 16-segment software-generated model. Base-to-apex LS, CS, and RS gradients were calculated as the peak gradient difference between averaged basal and apical LS, CS, and RS, respectively Fig. 2.

Concerning LS, data on myocardial strain were derived from 2-, 3- and 4-chamber long-axis views. Regarding RS and CS, data on myocardial strain was derived from apical, mid-ventricular, and basal short-axis views in all the patients. On all images, the epi- and endocardial borders were outlined in end-diastole. The basal level is the first slice that excludes the outflow tract throughout the cardiac cycle, as previously described.[24]

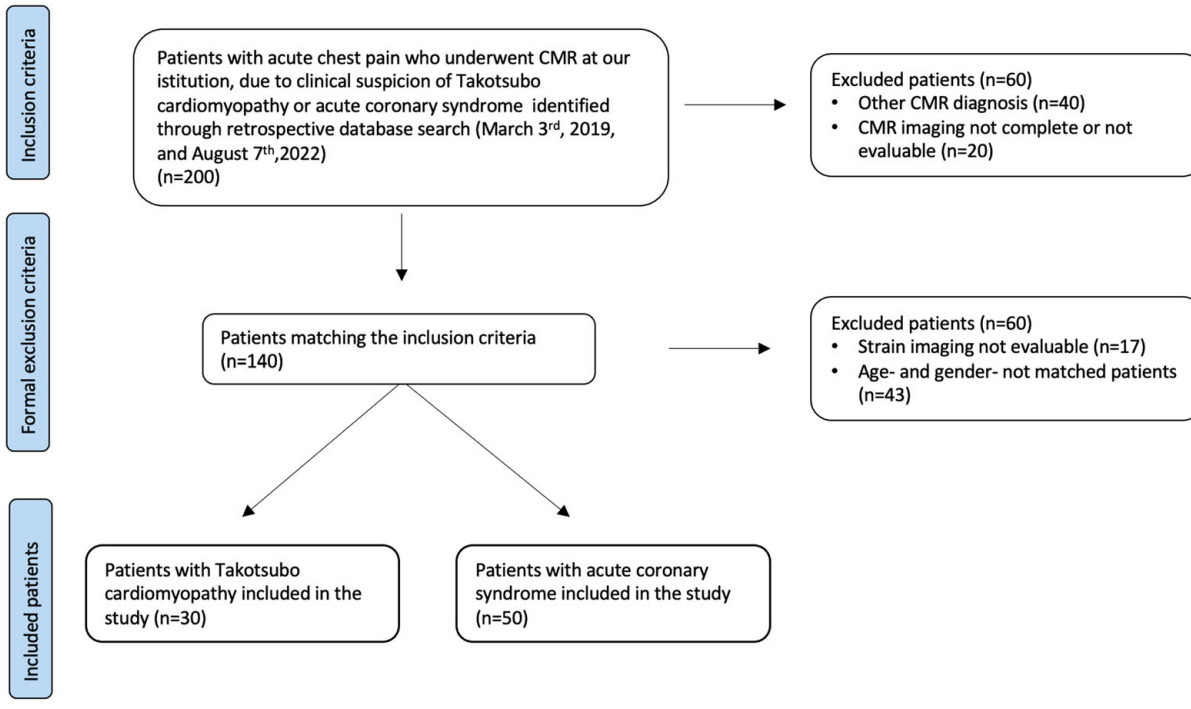

FIGURE 1. A flowchart demonstrating the application of inclusion and exclusion criteria. CMR indicates cardiovascular magnetic resonance. full color online

Copyright © 2023 Wolters Kluwer Health, Inc. All rights reserved.

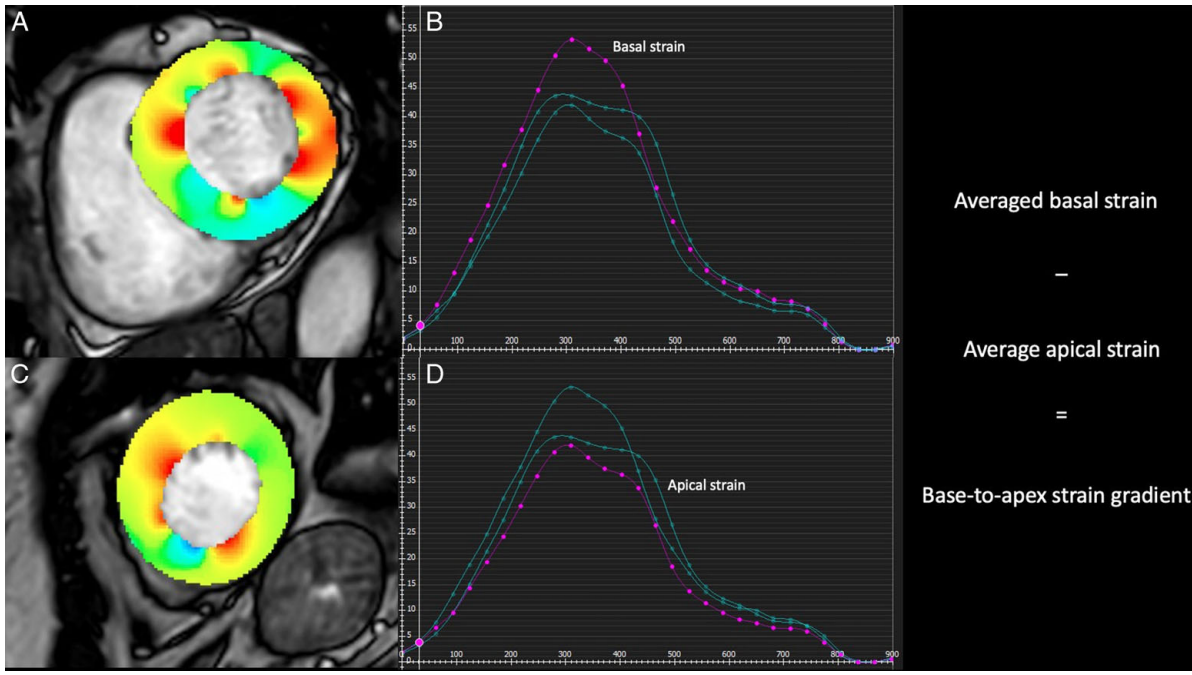

FIGURE 2. Cardiovascular magnetic resonance images of a 67-year-old male with Takotsubo cardiomyopathy. Basal short-axis cine bSSFP image with color myocardial radial strain map (A) and basal radial strain curve (B, purple curve). Apical short-axis cine bSSFP image with color myocardial radial strain map (C) and apical radial strain curve (D, purple curve). Base-to-apex radial strain gradients were calculated as the peak gradient difference between averaged basal and apical radial strain. The base-to-apex radial strain gradient was 13%. bSSFP indicates balanced steady-state free precession. full color online

Subsequently, an automatic computation was triggered, by which the applied software algorithm automatically outlined the border throughout the cardiac cycle. The quality of the tracking and contouring was visually validated and manually corrected when needed. For intraobserver analysis, 1 observer (R.C. with 5 years of experience in cardiovascular imaging) performed the analysis in a random subset of 20 patients.

For interobserver analysis, an additional blinded observer (M.P. with 6 years of experience in cardiovascular imaging) performed the same strain analysis in a random set of 20 patients.

T1 mapping and T2 mapping values were generated offline using the same dedicated CMR software (CVI42, Circle Cardiovascular Imaging Inc., Calgary, Canada). Epicardial and endocardial borders were manually traced and propagated through the image stack and manually corrected when needed.

T2-STIR images were evaluated using a qualitative visual assessment performed by 2 independent radiologist (R.C. with 5 years of experience in cardiovascular imaging, and M.P. with 6 years of experience in cardiovascular imaging) who were blinded to each other's results. The presence of T2-STIR signal abnormalities was established when there was agreement between the investigators.

LGE extension was qualitatively and quantitatively evaluated. Briefly, the location of the myocardial segment was evaluated and counted. The extension of LGE was obtained by tracing the epicardial and endocardial contours in each short-axis image. A region of interest was manually placed in the myocardium without LGE. The LGE was defined as myocardium with mean signal intensity >5 SDs greater than the reference region of interest.[25,26] The extent of LGE was expressed in the percentage of the LV mass.

Statistical Analysis

In this study, continuous data were described as the mean ± SD. The homogeneity of variance across groups was assessed through Levene's test. The normality of residuals was assessed through Kruskal-Wallis H, and Mann-Whitney U tests were used for comparison between groups of continuous variables, as appropriate. For categorical variables, we used the χ^2 test. A p-value <0.05 was considered statistically significant. Intraobserver and interobserver variability were assessed by intraclass correlation coefficients.

Binary logistic regression was used to assess the value of base-to-apex gradient parameters for the identification of TTC patients. CMR parameters were incorporated into univariable analysis as continuous variables, and significant predictors ($P<0.05$) were then included in multivariable analysis. To avoid collinearity, correlations between continuous variables were tested using Spearman correlation coefficients, and variables with $r>0.50$ were not included in the same multivariable model. Again, a receiver-operating characteristic (ROC) analysis was performed to calculate optimal thresholds and area under the curves. The Youden index was used to identify optimal cutoff values from the ROC curves. Sensitivities and specificities were calculated for these cutoff values with 95% confidence intervals.

Statistical analysis was performed using IBM SPSS Statistics version 25 (*SPSS* Inc., Chicago, IL, USA).

RESULTS

Patient Demographics and CMR Parameters

Overall, 80 patients were included in this study. Thirty patients with TTC were retrospectively enrolled (27 females; mean age 70.11 ± 9.72 y) and compared with 50 patients with AMI (39 females; mean age 67.72 ± 9.82 y). AMI patients showed a more prevalent presence and extent of myocardial fibrosis in comparison with TTC patients ($P = 0.001$ for both).

In TTC, CMR imaging demonstrated LGE in 9 (30%) patients when using a threshold of 5 SDs, with a pattern of LGE that involved the full thickness of the myocardium segments affected by wall motion abnormalities. AMI patients showed LGE in 47 (94%) when using a threshold of 5 SDs, with a transmural (15, 30%) or subendocardial (32, 64%) pattern of LGE.

No differences were found in T2-STIR, T1 mapping, and T2 mapping between TTC and AMI patients.

Baseline characteristics and CMR parameters of included patients are summarized in Table 1.

Myocardial Strain

The myocardial strain findings for regional LS, CS, RS, and base-to-apex gradient are reported in Table 1.

TABLE 1. Baseline characteristics and CMR parameters of included patients. The data are presented as mean ± SD for normally distributed quantitative variables and n (%) for qualitative variables

	Patients with TT	Patients with MI	*P*
Age	70.11 ± 9.72	67.72 ± 9.82	0.07
Sex (female)	27/30 (90)	39/50 (78)	0.07
LVEF	40.35 ± 16.65	46.12 ± 11.15	**0.02**
LVEDV/BSA	69 ± 15.90	109.91 ± 47.9	**0.001**
LVESV/BSA	30.77 ± 11.14	68.05 ± 41.52	**0.001**
LVSV/BSA	38.44 ± 12.40	40.13 ± 18.10	0.99
GRS	28.23 ± 9.31	19.83 ± 11	**0.001**
RS basal	39.13 ± 12.29	21.81 ± 10.78	**0.001**
RS mid	28.24 ± 10.59	19.03 ± 11.09	**0.001**
RS apical	25.08 ± 13.36	22.26 ± 16.1	0.22
GCS	-15.39 ± 7.89	-14.57 ± 5.32	0.15
CS basal	- 18.97 ±3.67	-13.67 ± 5	**0.001**
CS mid	- 16.64 ± 4.6	-12.27 ± 5.36	**0.001**
CS apical	-17.57 ± 6.32	-12.67 ± 8,12	**0.009**
GLS	-12.76 ± 3.31	-10.82 ± 4.92	0.062
LS basal	-15,36 ± 4.19	-10.46 ± 5.83	**0.001**
LS mid	-12.85 ±3.60	-10.37 ± 5.77	0.063
LS apical	-13.77 ± 3.91	-10.60 ± 6.12	**0.02**
Base-to-apex RS gradient	14.04 ± 15.50	-0.43 ± 11.59	**0.001**
Base-to-apex CS gradient	1.4 ± 5.43	-0.99 ± 6.49	0.47
Base-to-apex LS gradient	-1.5 ± 3.69	0.14 ± 2.71	0.054
LGE, g	10.40 ± 15.63	31.40 ± 13.68	0.001
LGE, n (%)	9/30(30)	47/50 (94)	0.001
T2-STIR	29/30 (96)	46/50 (92)	0.35
T2 mapping	65.11 ± 5.36	61.18 ± 9.08	0.12
T1 mapping	1121.58 ± 54.38	1130.11 ± 48.12	0.30

BSA indicates body surface area; CMR, cardiovascular magnetic resonance; CS, circumferential strain; EDV, end-diastolic volume; ESV, end-systolic volume; EF, ejection fraction; LS, longitudinal strain; LV, left ventricular;MI, myocardial infarction; LGE, late gadolinium enhancement; RS, radial strain; SV, stroke volume; TTC, Takotsubo cardiomyopathy; T2-STIR, T2-short tau inversion recovery.

Global RS was higher in TTC patients compared with the AMI group (28.23 ± 9.31 vs. 19.83 ± 11, $P = 0{,}001$). In contrast, global LS and CS did not differ between TTC and AMI patients (-12.76 ± 3.31 vs. -10.82 ± 4.92, $P = 0.062$: -15.39 ± 7.89 vs. -14.57 ± 5.32, $P = 0.15$)

By analyzing myocardial strain in the single segments, we observed that basal and mid RS were higher in TTC patients compared with the AMI group. Basal, mid, and apical CS were lower in TTC patients compared with the AMI group. Basal and apical LS were lower in TTC patients compared with the AMI group. While apical RS and mid LS did not differ between TTC and AMI.

Base-to-apex-gradients

The base-to-apex RS gradient was impaired in TTC patients compared with the AMI group (14.04 ± 15.50 vs. -0.43 ± 11.59, $P = 0.001$).

Conversely, base-to-apex LS and CS gradient did not differ between the AMI group and TTC patients (0.14 ± 2.71 vs. -1.5 ± 3.69, $P = 0.054$: -0.99 ± 6.49 vs ±1.4 ± 5.43, $P = 0.47$, respectively). Base-to-apex RS (OR 1.27; 95% CI 1.07, 1.51, $P = 0.005$) and CS (OR 1.44; 95% CI 1.04, 2.01, $P = 0.027$) gradients, global RS (OR 1.12; 95% CI 0.88, 1.43, $P = 0.016$), presence (OR 3.48; 95% CI 0.79, 23.21, $P = 0.001$) and extension (OR 0.91; 95% CI 0.87, 0.95, $P = 0.001$) of LGE were significantly associated with the presence of TTC in univariable analysis. Beyond the presence and extension of LGE, the base-to-apex RS gradient was the only independent discriminator between TTC and AMI (1.28; 95% CI 1.08, 1.52, $P = 0.006$; Table 2) in multivariate logistic regression analysis. On ROC analysis, a base-to-apex RS gradient of 4.9 predicted the presence of TTC with a sensitivity of 78%, specificity of 69%, and area under the curves of 0.793 (95% CI 0.682, 0.904), Fig. 3. The intraobserver and interobserver agreement was good for all base-to-apex strain gradient parameters. The intraclass correlation coefficients range from 0.881 to 0.959 for intraobserver agreement and from 0.812 to 0.861 for interobserver analysis.

DISCUSSION

The result of this study shows that the pronounced base-to-apex gradients pattern of RS may be an additional noncontrast CMR tool to discriminate between TTC and AMI. These findings suggested that base-to-apex RS gradients may be a marker of myocardial impairment in patients with TTC, proving a new insight into the pathology.

To the best of our knowledge, only a limited number of studies have evaluated CMR strain parameters in patients with TTC, and none have investigated the role of base-to-apex RS gradient.

Few previous studies have investigated myocardial strain impairment using CMR in patients with TTC,[5,20,27,28] demonstrating significantly lower LS, CS, and RS.[5,28] Eitel et al reported that all strain parameters were reduced in comparison with healthy subjects. The authors also evaluated left ventricle strain parameters in TTC patients in comparison with age-matched and sex-matched patients with anterior NSTEMI, reporting significantly reduced CS and LS values as well as a trend towards lower GRS in the TTC patients.[28] Cau et al in their retrospective study, investigated the role of CMR in patients with TTC compared with patients with acute myocarditis and the

TABLE 2. Univariate and Multivariate Logistic Regression of CMR Variables for Discrimination TTC and MI Group

	Univariable		Multivariable	
CMR variables	**OR (95%)**	***P***	**OR (95%)**	***P***
Base-to-apex RS	**1.27 (1.07–1.51)**	**0.005**	**1.28 (1.08–1.52)**	**0.006**
Base-to-apex CS	**1.44 (1.04–2.01)**	**0.027**	1.30 (0.86–1.96)	0.20
Base-to-apex LS	0.85 (0.69–1.05)	0.15	0.68 (0.40–1.11)	0.16
Global RS	**1.12 (0.88–1.43)**	**0.016**	1.08 (0.90–1.35)	0.32
Global CS	1.04 (0.90–1.21)	0.51	0.95 (0.74–1.21)	0.69
Global LS	1.06 (0.90–1.26)	0.44	1.07 (0.57–1.72)	0.98
LGE	3,48 (0.79–23.21)	**0.001**	5.86 (1.63–12.86)	**0.001**
LGE, g	0.91 (0.87–0.95)	**0.001**	0.86 (0.79–0.93)	**0.001**
T2-STIR	0.36 (0.04–3.62)	0,36	1.29 (0.10–15.63)	0.83
T2 mapping	1.09 (0.95–1.19)	0.06	1.04 (0.89–1.21)	0.59
T1 mapping	0.95 (0.83–1.07)	0.43	0.99 (0.83–1.18)	0.93

CMR indicates cardiovascular magnetic resonance; CS, circumferential strain; LGE, late gadolinium enhancement; LS, longitudinal strain; OR, odd ratio; RS, radial strain; TTC, Takotsubo cardiomyopathy; T2-STIR, T2-short tau inversion recovery.

control group, demonstrating that LS, CS, and RS were significantly lower in TTC in comparison with other groups. In particular, the authors reported significantly higher values of basal RS.[5] Backhaus et al investigated the influence of CMR dyssynchrony and rotational mechanics in TTC and reported that circumferential uniformity ratio estimates were initially reduced compared with controls ($P = 0.001$). In addition, the authors reported that radial uniformity ratio estimates ($P = 0.045$) and circumferential uniformity ratio estimates ($P = 0.001$) accurately discriminate between different ballooning patterns with the highest dyssynchrony associated with apical ballooning.[29] In comparison with the previous above-mentioned studies, we investigated novel CMR parameters in TTC patients, namely base-to-apex strain gradient.

The base-to-apex gradients have also been analyzed in other cardiomyopathies. A loss of base-to-apex gradient has been shown to identify patients with Fabry disease and healthy subjects.[30] Phelan et al described regional LS patterns in patients with cardiac amyloidosis, reporting regional variations in LS from base to apex, with a relative sparing of apical segments.[31]

In our study, we found that there was a significant difference in base-to-apex RS gradient between TTC patients and AMI. Physiologically, in the ventricle, the LS, CS, and RS increase from basal to apical segments[32]; this could be explained by the difference in myocardial architecture into 3 distinctive layers with different fibber orientations.[15] The potential pathophysiological mechanism determining the pronounced base-to-apex RS gradients in TTC has not yet been established. Lee et al reported an impairment of base-to-apex RS gradients in TTC patients, suggesting that an increase in basal segment contractility was caused only by a higher value of RS, not by an increase in longitudinal and circumferential strain.[21] Conversely, base-to-apex LS and CS gradients were not significantly impaired in TTC patients, similar to a prior study that evaluated strain using echocardiography.[21]

The data from our study suggests that the base-to-apex gradient could serve as a supportive noncontrast CMR

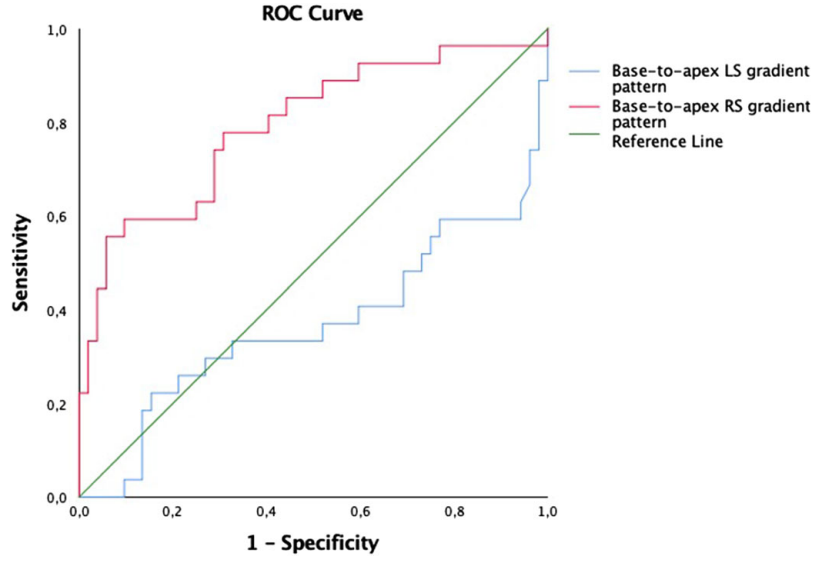

FIGURE 3. ROC curves illustrate the diagnostic performance of base-to-apex RS (red line) and LS (green line) gradient patterns to discriminate patients with Takotsubo cardiomyopathy from patients with anterior wall myocardial infarction. LS indicates longitudinal strain; ROC, receiver-operating characteristic; RS, radial strain. full color online

diagnostic feature in distinguishing between TTC and AMI. Integrating contrast-free strain analysis into clinical practice has the potential to improve the utility of CMR examinations in a specific group of patients.

A major limitation of this research is the relatively small number of patients and the retrospective selection of the patients' cohort. However, we enrolled exclusively TTC patients with the apical type. The promising results of our study prompt further study (eg, EVOLUTION registry[33]), including larger cohorts to confirm our findings. Moreover, the predictive value of myocardial strain for adverse cardiovascular events has not been assessed in our study at follow-up. Finally, the impairment in myocardial strain in patients with TTC would have been probably different if CMR was performed within a shorter period of time, ideally the same day of hospital admission.

In conclusion, our findings suggest that the pattern of LV regional strain abnormalities assessed using CMR may be an additional noncontrast tool in refining TTC diagnosis.

Additional studies with a larger number of patients are needed to confirm the usefulness of these advanced CMR tools in TTC patients.

REFERENCES

1. Ghadri J-R, Wittstein IS, Prasad A, et al. International Expert Consensus Document on Takotsubo Syndrome (Part I): clinical characteristics, diagnostic criteria, and pathophysiology. *Eur Heart J*. 2018;39:2032–2046.
2. Ghadri J-R, Wittstein IS, Prasad A, et al. International Expert Consensus Document on Takotsubo Syndrome (Part II): Diagnostic workup, outcome, and management. *Eur Heart J*. 2018;39:2047–2062.
3. Ono R, Falcão LM. Takotsubo cardiomyopathy systematic review: pathophysiologic process, clinical presentation and diagnostic approach to Takotsubo cardiomyopathy. *Int J Cardiol*. 2016;209:196–205.
4. Weiner MM, Asher DI, Augoustides JG, et al. Takotsubo cardiomyopathy: a clinical update for the cardiovascular anesthesiologist. *J Cardiothorac Vasc Anesth*. 2017;31:334–344.
5. Cau R, Bassareo P, Deidda M, et al. Could CMR Tissue-Tracking and Parametric Mapping Distinguish Between Takotsubo Syndrome and Acute Myocarditis? A Pilot Study. *Acad Radiol Published online*. 2021;■:■. http://www.sciencedirect.com/science/article/pii/S1076633221000155
6. Cau R, Bassareo P, Caredda G, et al. Atrial strain by feature-tracking cardiac magnetic resonance imaging in Takotsubo cardiomyopathy. Features, Feasibility, and Reproducibility. *Can Assoc Radiol J = J l'Association Can des Radiol* Published online2021;■:8465371211042497.
7. Jensch P-J, Stiermaier T, Eitel I. Takotsubo Syndrome-Is there a need for CMR? *Curr Heart Fail Rep*. 2021;18:200–210.
8. Eitel I, von Knobelsdorff-Brenkenhoff F, Bernhardt P, et al. Clinical characteristics and cardiovascular magnetic resonance findings in stress (Takotsubo) cardiomyopathy. *JAMA*. 2011; 306:■. doi:10.1001/jama.2011.992
9. 2022 ESC Guidelines for the management of patients with ventricular arrhythmias and the prevention of sudden cardiac death: developed by the task force for the management of patients with ventricular arrhythmias and the prevention of sudden cardiac death. *Eur Heart J* Published online, 2022:■: ehac262. doi:10.1093/eurheartj/ehac262
10. McDonagh TA, Metra M, Adamo M, et al. 2021 ESC Guidelines for the diagnosis and treatment of acute and chronic heart failure: developed by the task force for the diagnosis and treatment of acute and chronic heart failure of the European Society of Cardiology (ESC) With the special contributio. *Eur Heart J*. 2021;42:3599–3726.
11. Cau R, Bassareo P, Cherchi V, et al. Early diagnosis of chemotherapy-induced cardiotoxicity by cardiac MRI. *Eur J Radiol*. 2020;130:109158.
12. Cau R, Solinas C, De Silva P, et al. Role of cardiac MRI in the diagnosis of immune checkpoint inhibitor-associated myocarditis. *Int J Cancer*. 2022;■:■. Published online. doi:10.1002/ijc.34169
13. Cau R, Bassareo PP, Mannelli L, et al. Imaging in COVID-19-related myocardial injury. *Int J Cardiovasc Imaging* Published online2020;■:■. doi:10.1007/s10554-020-02089-9
14. Cau R, Cherchi V, Micheletti G, et al. Potential role of artificial intelligence in cardiac magnetic resonance imaging. *J Thorac Imaging*. 2021 142–148.
15. Scatteia A, Baritussio A, Bucciarelli-Ducci C. Strain imaging using cardiac magnetic resonance. *Heart Fail Rev*. 2017;22: 465–476.
16. Xu J, Yang W, Zhao S, et al. State-of-the-art myocardial strain by CMR feature tracking: clinical applications and future perspectives. *Eur Radiol*. 2022;32:5424–5435.
17. Fong LCW, Lee NHC, Poon JWL, et al. Prognostic value of cardiac magnetic resonance derived global longitudinal strain analysis in patients with ischaemic and non-ischaemic dilated cardiomyopathy: a systematic review and meta-analysis. *Int J Cardiovasc Imaging*. 2022;38:2707–2721.
18. Bratis K. Cardiac Magnetic Resonance in Takotsubo Syndrome. *Eur Cardiol*. 2017;12:58–62.
19. Cau R, Loewe C, Cherchi V, et al. Atrial impairment as a marker in discriminating between takotsubo and acute myocarditis using cardiac magnetic resonance. *J Thorac Imaging*. ■:■:■; Published online 9900. https://journals.lww.com/thoracicimaging/Fulltext/9900/Atrial_Impairment_as_a_Marker_in_Discriminating.2.aspx
20. Cau R, Pisu F, Porcu M, et al. Machine learning approach in diagnosing Takotsubo cardiomyopathy: the role of the combined evaluation of atrial and ventricular strain, and parametric mapping. *Int J Cardiol*. 2022;■:■.Published online. doi:10.1016/j.ijcard.2022.11.021
21. Lee M. Time course of functional recovery in takotsubo (stress) cardiomyopathy: a serial speckle tracking echocardiography and electrocardiography study. *J Cardiovasc imaging*. 2020;28: 50–60.
22. Kobayashi Y, Okura H, Kobayashi Y, et al. Left ventricular myocardial function assessed by three-dimensional speckle tracking echocardiography in Takotsubo cardiomyopathy. *Echocardiography*. 2017;34:523–529.
23. Lyon AR, Bossone E, Schneider B, et al. Current state of knowledge on Takotsubo syndrome: a position statement from the taskforce on Takotsubo syndrome of the heart failure association of the European Society of Cardiology. *Eur J Heart Fail*. 2016;18:8–27.
24. Liu H, Yang D, Wan K, et al. Distribution pattern of left-ventricular myocardial strain analyzed by a cine MRI based deformation registration algorithm in healthy Chinese volunteers. *Sci Rep*. 2017;7:45314.
25. Schulz-Menger J, Bluemke DA, Bremerich J, et al. Standardized image interpretation and post-processing in cardiovascular magnetic resonance - 2020 update. *J Cardiovasc Magn Reson*. 2020;22:19.
26. Cau R, Bassareo P, Cademartiri F, et al. Epicardial fat volume assessed with cardiac magnetic resonance imaging in patients with Takotsubo cardiomyopathy. *Eur J Radiol*. 2023;160:110706.
27. Stiermaier T, Busch K, Lange T, et al. Prognostic value of different CMR-based techniques to assess left ventricular myocardial strain in Takotsubo Syndrome. *J Clin Med*. 2020; 9:3882.
28. Stiermaier T, Lange T, Chiribiri A, et al. Left ventricular myocardial deformation in Takotsubo syndrome: a cardiovascular magnetic resonance myocardial feature tracking study. *Eur Radiol*. 2018;28:5160–5170.
29. Backhaus SJ, Stiermaier T, Lange T, et al. Temporal changes within mechanical dyssynchrony and rotational mechanics in Takotsubo syndrome: a cardiovascular magnetic resonance imaging study. *Int J Cardiol*. 2018;273:256–262.

30. Mathur S, Dreisbach JG, Karur GR, et al. Loss of base-to-apex circumferential strain gradient assessed by cardiovascular magnetic resonance in Fabry disease: relationship to T1 mapping, late gadolinium enhancement and hypertrophy. *J Cardiovasc Magn Reson*. 2019;21:45.
31. Phelan D, Collier P, Thavendiranathan P, et al. Relative apical sparing of longitudinal strain using two-dimensional speckle-tracking echocardiography is both sensitive and specific for the diagnosis of cardiac amyloidosis. *Heart*. 2012;98:1442–1448.
32. Sugimoto T, Dulgheru R, Bernard A, et al. Echocardiographic reference ranges for normal left ventricular 2D strain: results from the EACVI NORRE study. *Eur Hear J - Cardiovasc Imaging*. 2017;18:833–840.
33. Cau R, Muscogiuri G, Pisu F, et al. Exploring the EVolution in PrognOstic CapabiLity of MUltisequence Cardiac MagneTIc ResOnance in PatieNts affected by Takotsubo cardiomyopathy based on machine learning analysis design and rationale of the EVOLUTION Study. ■. 2023;00:1–8.

AQ13